FR9326252

DRFC/CAD EUR-CEA-FC-1475

ON THE DYNAMICS OF THE POWER SPECTRUM DURING LOWER HYBRID CURRENT DRIVE IN TOKAMAKS

J. P. Bizarro

Janvier 1993

CEA EURATOM

ASSOCIATION EURATOM-C.E.A.
DEPARTEMENT DE RECHERCHES
SUR LA FUSION CONTROLEE
C.E.N./CADARACHE
13108 SAINT PAUL LEZ DURANCE CEDEX

ON THE DYNAMICS OF THE POWER SPECTRUM DURING LOWER HYBRID CURRENT DRIVE IN TOKAMAKS*

JOÃO P. BIZARRO

Département de Recherches sur la Fusion Contrôlée, Association Euratom-CEA,

Centres d' Etudes de Cadarache, 13108 St. Paul lez Durance Cedex, France

ABSTRACT

An investigation is provided on the propagation and absorption of the power spectrum during lower hybrid current drive in tokamaks. A combined ray tracing and Fokker-Planck code is utilized and stochastic effects induced by toroidicity are correctly taken into account by using a large number of rays. It is shown that when strong wave damping prevails the absorbed spectrum is very similar in shape to the launched one, although some broadening and shifting in parallel wave index generally occur, and power deposition is localized. If the wave damping is weak and stochastic effects are important, rays end up sweeping the entire plasma cross-section, power deposition turns out to be extended, and the absorbed spectrum is much broader than the launched one.

* Preprint of a letter submitted to Nuclear Fusion

Ray tracing has been extensively used to study the propagation and absorption of the lower hybrid (LH) wave in tokamaks and to investigate the importance of the variations in parallel wave index due to the poloidal symmetry breaking in toroidal geometry [1-7]. Such variations are in general large enough to enable waves injected at low parallel wave index to upshift and to Landau damp on electrons, thus providing a mechanism for bridging the spectral gap typical of LH current drive [8,9]. Alternative approaches have been proposed [10-12] but they are still far from having the degree of assessment that ray tracing has acquired. Moreover, ray tracing has been very effective in modeling LH current drive experiments when coupled with Fokker-Planck calculations [8,9]. One of the main properties of the ray equations in toroidal geometry is the possibility they have of exhibiting intrinsic stochastic behavior [1,6,10,13]. It is clear that ray tracing may correctly account for stochastic effects only when a sufficiently large number of rays is used, in which case ray tracing may be regarded as a Monte-Carlo-like manner of propagating the LH wave. It is the purpose of this letter to use ray tracing to provide an investigation of the dynamics of the power spectrum during LH current drive in situations where stochastic effects are important. Attention is paid to the influence of the balance between the wave damping and the stochastic divergence of nearby ray trajectories in governing the spectrum dynamics and in establishing the characteristics of the LH power deposition patterns.

A well documented and assessed code [8,9,14] has been utilized to carry out the proposed study. It couples three distinct parts: a one-dimensional radial transport module that evolves the thermal plasma [9], a multiple-pass toroidal ray tracing and power deposition module [8,9], and a one-dimensional (in parallel momentum) Fokker-Planck module [8,9], where two-dimensional effects are incorporated through analytic estimates of the perpendicular temperature [15] and through corrections due to trapped particles [16]. The electron distribution function is calculated in a quasilinear manner by self-consistently iterating the power deposition and the Fokker-Planck calculations [8,9,14]. Feedback stabilization of the plasma current and radial diffusion of the LH driven current density are also included [14]. Accurate representations of the poloidal extent of the

antenna and of its radiated spectrum are used, thus ensuring that the initial conditions provided to the ray tracing calculation correctly reproduce the injected LH power distribution both in poloidal angle, θ, and in parallel wave index, $n_{//}$.

The analysis given below has been performed for a combined ohmic-LH steady state typical of the current drive experiment in TORE SUPRA [17]. The basic plasma characteristics are: helium gas, major radius $R_0 = 2.34$ m, minor radius $a = 0.78$ m, magnetic field on axis $B_0 = 3.9$ T, central electron density $n_{e0} = 5.3 \times 10^{19}$ m^{-3}, volume-averaged electron density $\langle n_e \rangle = 3.3 \times 10^{19}$ m^{-3}, central electron temperature $T_{e0} = 3.1$ keV, volume-averaged electron temperature $\langle T_e \rangle = 1.5$ keV, ion effective charge $Z_{eff} = 2.8$, loop voltage $V_{loop} = 0.57$ V, and toroidal current $I_p = 1.6$ MA, 19% of which is of non-inductive nature. The wave frequency is $\omega/2\pi = 3.7$ GHz and the total LH injected power is $P_{in} = 2.46$ MW. The power P_{in} is equally divided into the four θ values corresponding to the poloidal locations of the four rows of waveguides that form the antenna, which is installed in the low field side of the equatorial mid-plane and which extends roughly 0.38 radians in the θ direction. The same power spectrum is launched from each θ value and only the two main lobes of the spectrum radiated by the antenna are retained. The negative lobe ($n_{//} < 0$) is peaked at $n_{//} = -5.62$ and is described using 21 rays, whereas the positive lobe ($n_{//} > 0$) is peaked at $n_{//} = 1.59$ and is described using 100 rays. This makes a total of 84 rays traced with $n_{//} < 0$ and of 400 rays traced with $n_{//} > 0$. Practically all the power in the positive lobe (68% of P_{in}) is injected with $n_{//}$ values that are not accessible to the plasma center [6,18], since for the present set of parameters central penetration of the LH wave requires $|n_{//}| \gtrsim 1.7$.

During the integration of the ray equations, ray data are stored each time the increment in the absolute value of ρ is greater than or equal to 0.015, where ρ stands for the normalized radial flux surface coordinate ($\rho = 1$ at the plasma minor radius). Using such data and if τ designates a normalized time variable ($\tau = 1$ when the total power carried by the rays falls below 1% of P_{in}), time evolution calculations of the launched spectrum up to $\tau = \tau'$ have been performed on a 101×101 mesh in

$(0 \le \tau \le \tau') \times (1 \le |n_{//}| \le 7)$, and power deposition calculations have been performed on a 101×101 mesh in $(0 \le \rho \le 1) \times (1 \le |n_{//}| \le 7)$.

The projection in the (ρ,θ) polar plane of the ray trajectories before complete damping occurs are depicted in Fig. 1. It is striking to see how differently the two lobes behave. The reasons why this happens have to do with the fact that the dynamics of the high-$|n_{//}|$ negative lobe is characterized by strong wave damping, whereas the dynamics of the low-$|n_{//}|$ positive lobe is dominated by stochastic effects. While rays launched with $n_{//} < 0$ move coherently, rays launched with $n_{//} > 0$ suffer a stochastic divergence and end up completely filling the tokamak cavity. Moreover, rays with $n_{//} > 0$ do go through the plasma center even if initially most of them have $n_{//} \lesssim 1.7$. Only apparently this can be considered as surprising, since it is well known that ray stochasticity can greatly alter the accessibility constraints on the launched spectrum [6]. The time evolution of the LH spectral density, $S_{LH}(\tau,n_{//})$, is reported in Fig. 2. The characteristic damping times are very different for the negative and positive lobes. Furthermore, the former essentially keeps its shape and propagates in a regular manner, whereas the latter is distorted and broadened. Such distinct behaviours reflect themselves in the way the LH power is damped on the plasma electron population. The absorbed power density per unit interval of $n_{//}$ due to electron Landau damping, $W_{ELD}(\rho,n_{//})$, can be seen in Fig. 3. Quite naturally, the power deposition pattern associated with the negative lobe is highly localized as compared to the extended pattern associated with the positive lobe. The picture that may thus be retained when the ray dynamics is dominated by stochastic effects is the one of a diffusion of the LH energy density in the $(\rho,n_{//})$ space. The absorbed and the launched spectra, $S_{ELD}(n_{//}) = (2\pi a)^2 R_0 \int_0^1 W_{ELD}(\rho',n_{//})\,\rho'\,d\rho'$ and $S_{LH}(0,n_{//})$ respectively, are plotted in Fig. 4. Comparing the two, the negative lobe of the absorbed spectrum is slightly broadened and upshifted in $|n_{//}|$, and as might have been expected the major modifications take place for the positive lobe, which is strongly broadened in the high-$n_{//}$ side. This last result is in agreement with a previous work where a different approach has been followed [19].

In conclusion, when strong wave damping prevails the power spectrum behaves regularly, although some broadening and shifting in parallel wave index generally occur. Power deposition is localized and the absorbed spectrum is very similar in shape to the launched one. If the wave damping is weak and stochastic effects are important, rays end up completely sweeping the plasma cross-section and the spectrum dynamics becomes diffusive-like. Power deposition turns out to be extended and the absorbed spectrum is much broader than the launched one.

ACKNOWLEDGEMENTS

The author is grateful to Dr. Paul T. Bonoli and Dr. Vladimir Fuchs for kindly providing the original code, and to Dr. Kenneth Kupfer for fruitful discussions. Useful comments on the manuscript by Dr. Gerardo Giruzzi, Dr. Didier Moreau, and Dr. Yves Peysson are also acknowledged.

The present letter is part of the work carried out by the author in fulfilment of the requirements for obtaining the Doctorate degree (Université de Provence, Aix-Marseille I). The author was supported by the Commission of the European Communities under Euratom grant B 89000563.

REFERENCES

[1] WERSINGER, J.-M., OTT, E., FINN, J. M., Phys. Fluids **21** (1978) 2263.

[2] COLESTOCK, P. L., KULP, J. L., IEEE Trans. Plasma Sci. **PS-8** (1980) 71.

[3] BARANOV, Yu. F., FEDOROV, V. I., Nucl. Fusion **20** (1980) 1111.

[4] IGNAT, D. W., Phys. Fluids **24** (1981) 1110.

[5] BERNABEI, S., IGNAT, D. W., Nucl. Fusion **22** (1982) 735.

[6] BONOLI, P. T., OTT, E., Phys. Fluids **25** (1982) 359.

[7] BRAMBILLA, M., Comput. Phys. Rep. **4** (1986) 71.

[8] BONOLI, P. T., ENGLADE, R. C., Phys. Fluids **29** (1986) 2937.

[9] BONOLI, P. T., PORKOLAB, M., TAKASE, Y., KNOWLTON, S. F., Nucl. Fusion **28** (1988) 991.

[10] MOREAU, D., RAX, J. M., SAMAIN, A., Plasma Phys. Controlled Fusion **31** (1989) 1895.

[11] MOREAU, D., PEYSSON, Y., RAX, J. M., SAMAIN, A., DUMAS, J. C., Nucl. Fusion **30** (1990) 97.

[12] PEREVERZEV, G. V., Nucl. Fusion **32** (1992) 1091.

[13] KUPFER, K., MOREAU, D., Nucl. Fusion **32** (1992) 1845.

[14] FUCHS, V., SHKAROFSKY, I. P., CAIRNS, R. A., BONOLI, P. T., Nucl. Fusion **29** (1989) 1479.

[15] FUCHS, V., CAIRNS, R. A., SHOUCRI, M. M., HIZANIDIS, K., BERS, A., Phys. Fluids **28** (1985) 3619.

[16] EHST, D. A., KARNEY, C. F., Nucl. Fusion **31** (1991) 1933.

[17] MOREAU, D., TORE SUPRA Team, Phys. Fluids B **4** (1992) 2165.

[18] GOLANT, V. E., Sov. Phys. Tech. Phys. **16** (1972) 1980.

[19] PEYSSON, Y., FROISSARD, P., BIZARRO, J. P., BRUSATI, M., CARRASCO, J., EKEDAHL, A., GORMEZANO, C., HOANG, G. T., JACQUINOT, J., KUPFER, K., LITAUDON, X., MOREAU, D., PASINI, D., RAX, J. M., RIGAUD, D., RIMINI, F., in

Radiofrequency Heating and Current Drive of Fusion Devices (Proc. Eur. Top. Conf. Brussels, 1992), Vol. 16E, European Physical Society (1992) 217.

FIGURE CAPTIONS

FIG. 1. Projection in the (ρ,θ) polar plane of the ray trajectories for: (a) $n_{//} < 0$ and (b) $n_{//} > 0$. The outer circle corresponds to $\rho = 1.1$.

FIG. 2. Time evolution of the power spectrum up to: (a) $\tau = 0.05$ and (b) $\tau = 1$.

FIG. 3. Absorbed power density per unit interval of $n_{//}$.

FIG. 4. Absorbed and launched spectra.

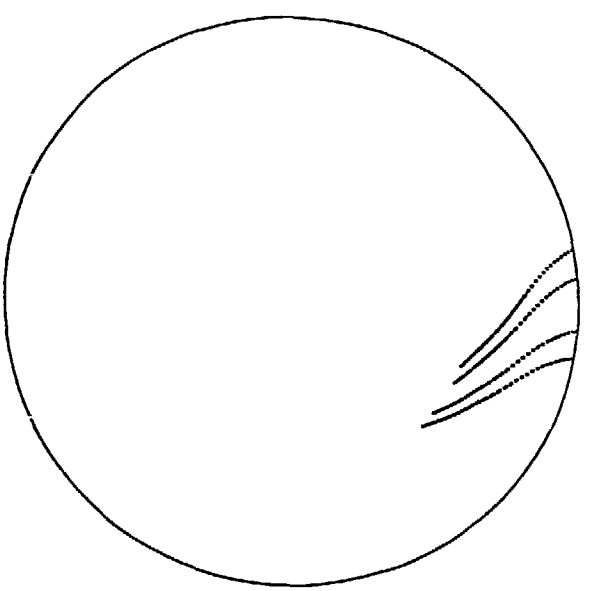

(a)

$n_{//} < 0$

FIGURE 1 (a)

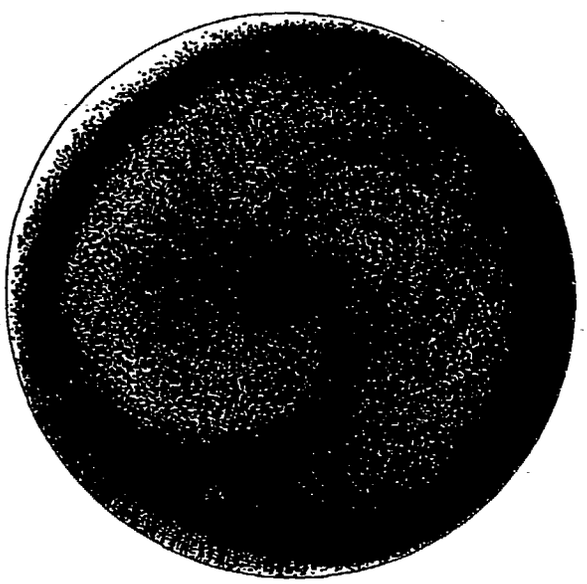

(b)

$n_{//} > 0$

FIGURE 1 (b)

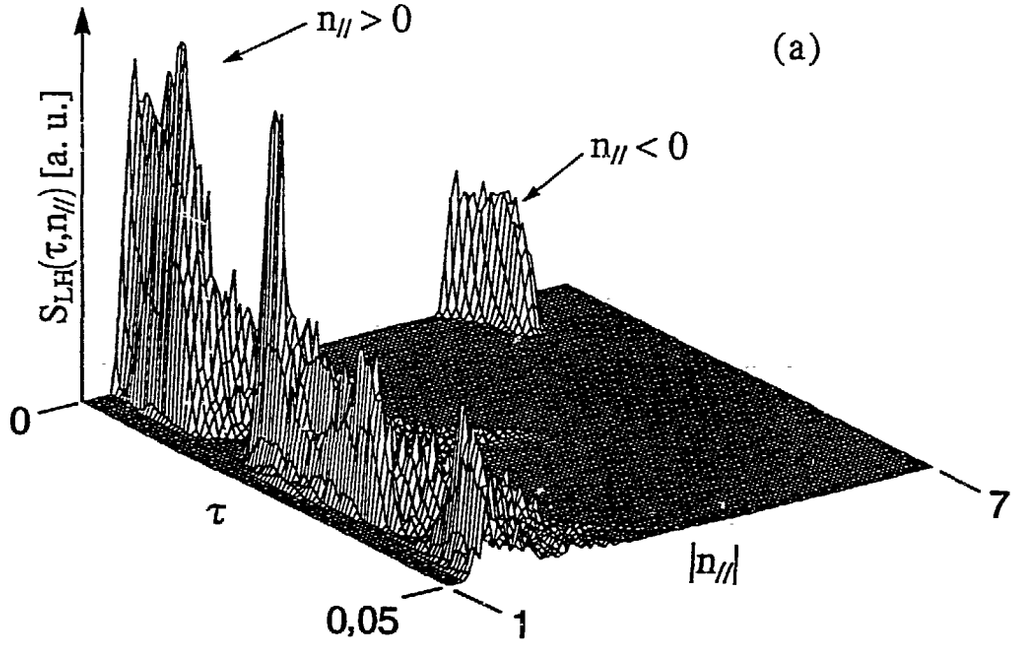

FIGURE 2 (a)

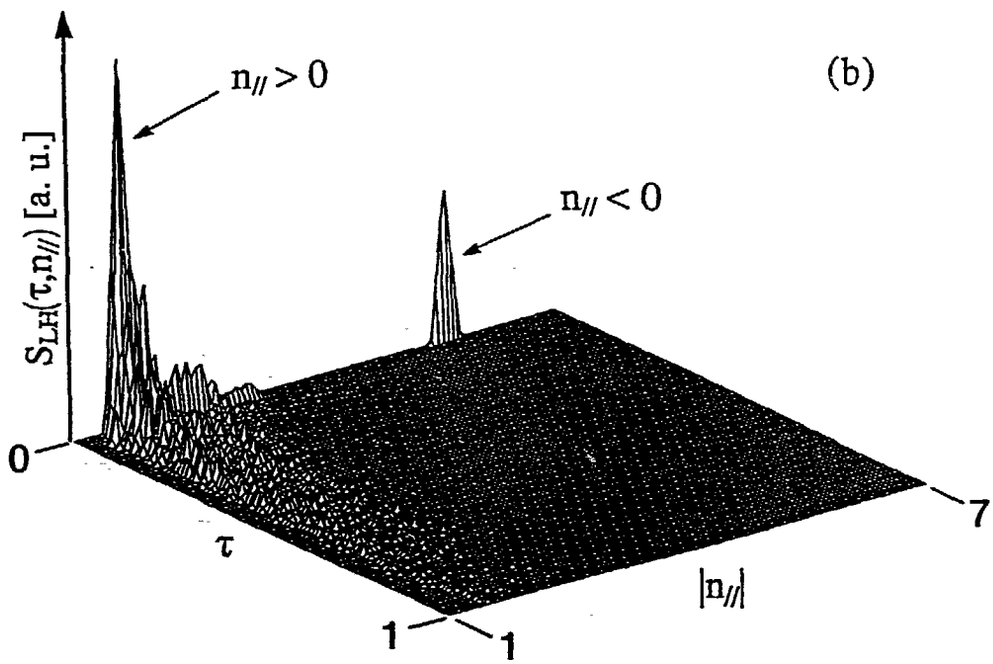

FIGURE 2 (b)

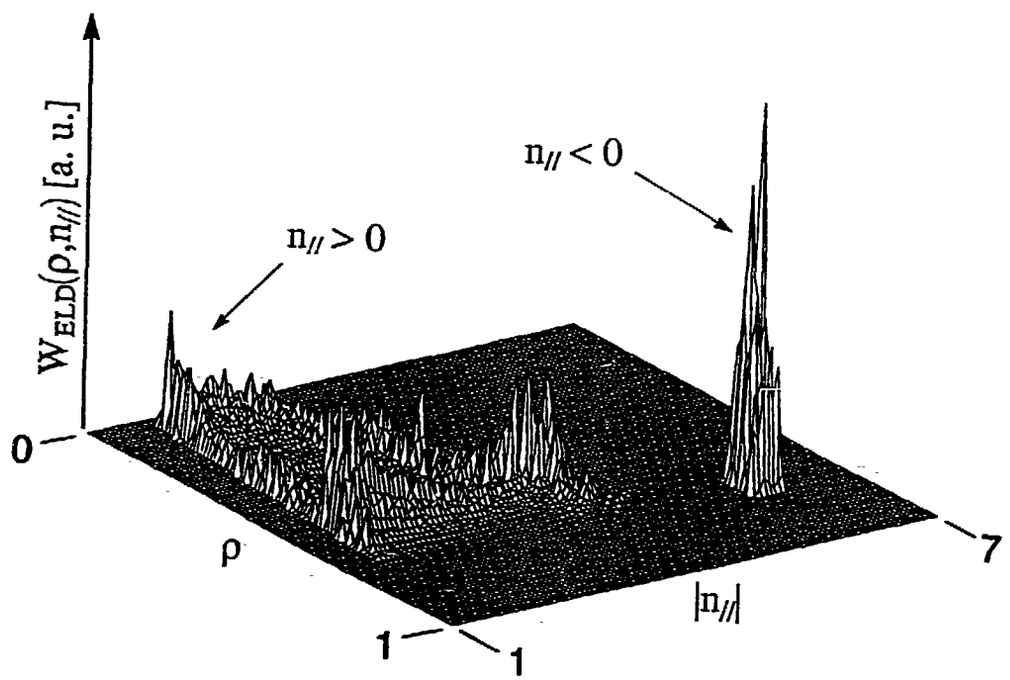

FIGURE 3

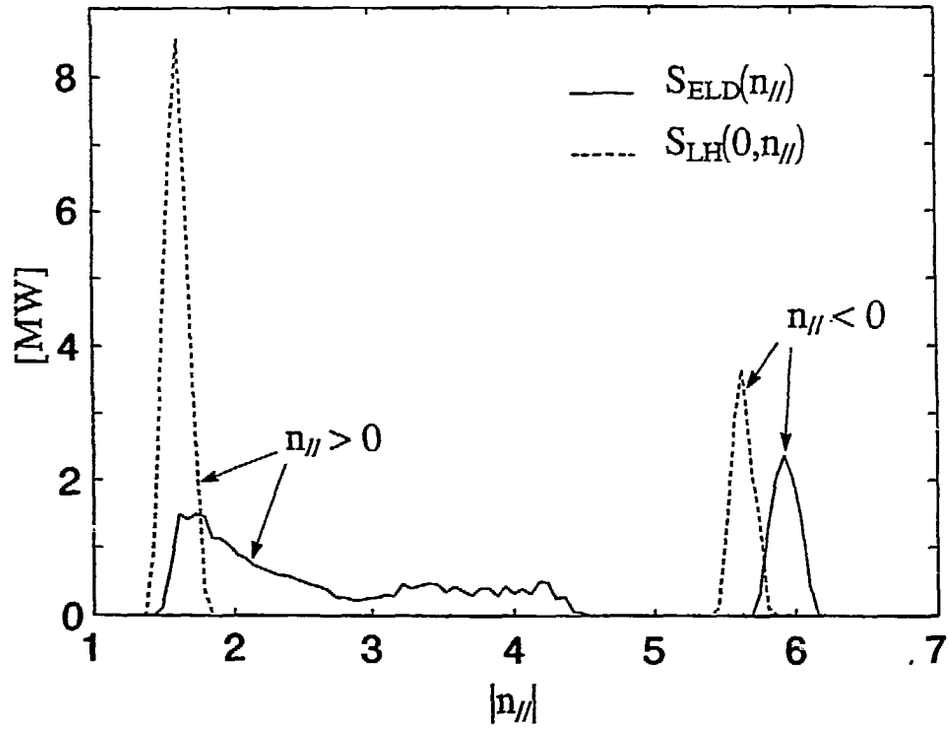

FIGURE 4